Forced periodic expression of G_1 cyclins phase-locks the budding yeast cell cycle

G. Charvin[a,b,1], F. R. Cross[a], and E. D. Siggia[b]

[a]Laboratory of Yeast Molecular Genetics and [b]Center for Studies in Physics and Biology, The Rockefeller University, New York, NY 10021

Edited by Robert H. Austin, Princeton University, Princeton, NJ, and approved February 17, 2009 (received for review September 16, 2008)

Phase-locking (frequency entrainment) of an oscillator, in which a periodic extrinsic signal drives oscillations at a frequency different from the unperturbed frequency, is a useful property for study of oscillator stability and structure. The cell cycle is frequently described as a biochemical oscillator; however, because this oscillator is tied to key biological events such as DNA replication and segregation, and to cell growth (cell mass increase), it is unclear whether phase locking is possible for the cell cycle oscillator. We found that forced periodic expression of the G_1 cyclin *CLN2* phase locks the cell cycle of budding yeast over a range of extrinsic periods in an exponentially growing monolayer culture. We characterize the behavior of cells in a pedigree using a return map to determine the efficiency of entrainment to the externally controlled pulse. We quantify differences between mothers and daughters and how synchronization of an expanding population differs from synchronization of a single oscillator. Mothers only lock intermittently whereas daughters lock completely and in a different period range than mothers. We can explain quantitative features of phase locking in both cell types with an analytically solvable model based on cell size control and how mass is partitioned between mother and daughter cells. A key prediction of this model is that size control can occur not only in G_1, but also later in the cell cycle under the appropriate conditions; this prediction is confirmed in our experimental data. Our results provide quantitative insight into how cell size is integrated with the cell cycle oscillator.

cell size control | phase locking

Synchronization of 2 oscillators is a well-understood physical phenomenon, and it occurs in multiple biological systems, such as entrainment of the circadian oscillator to the light–dark cycle or electrical synchronization of heart cells (1, 2). The mathematical theory of oscillating systems predicts that any 2 oscillators with sufficiently similar periods will phase lock (i.e., oscillate with a fixed relative phase) when coupled together and thus oscillate with a common frequency (3). This is true for all systems described by smooth nonlinear deterministic equations. The phase locked state is stable against perturbations, and thus persists in the presence of weak ''noise'' such as produced by small numbers of molecules in biochemical systems. A phase locked system is less noisy than its components (4, 5). When a rare fluctuation in the nondeterministic elements exceeds the stability domain, the relative phase of the coupled oscillators ''slips'' by 1 cycle and then returns to synchrony.

Phase locking of an oscillator to an external periodic signal is completely analogous to locking between oscillators, and has the additional benefit that the frequency is under direct experimental control. The stability of the phase locked state implies that a nonlinear oscillator will lock for a range of external periods, and the magnitude of that range of periods is a direct measure of oscillator stability.

The budding yeast cell cycle is well understood genetically, and is frequently described as a biochemical oscillator driven by waves of cyclin-dependent kinase mediated phosphorylations combined with periodic dephosphorylations and protein degradations (6); however, the dynamical systems properties of this oscillator remain to be characterized in any formal way, despite the existence of a powerful set of tools for oscillator characterization developed for simple physical systems.

Cell growth or mass increase is exponential in budding yeast, and not dependent on cell cycle position; coordination of growth and division occurs by a specific delay in cell cycle initiation (Start) in small cells (7–9). Budding yeast divide asymmetrically, with a larger mother typically producing a smaller daughter; this difference may largely (but not entirely) account for detection of size control in daughters but not in mothers (9, 10). If the ratio of mother and daughter masses is fixed at division then their respective cycle times are dictated by the exponential rate constant for cell growth. In addition, numerous coupling mechanisms (checkpoints) coordinate DNA replication, spindle integrity and nuclear positioning. For these reasons, it is unclear whether the yeast cell cycle can be stably phase-locked to a different period by any manipulation. A previous theoretical analysis of this problem suggested that daughter but not mother cells could be phase-locked by pulses of G_1 cyclin expression, under the specific constraint that all mass increase after bud emergence went to the new daughter cell body (11).

We examined the potential for phase-locking the budding yeast cell cycle using periodic pulses of the G_1 cyclin *CLN2*, and quantify this behavior by following the size and division and budding times of a growing colony of yeast cells over 8 generations in a microfluidic flow cell, that allows for precise control of the environment (including rapid addition and removal of inducers of gene expression) while keeping the colony flat for imaging (12). Under periodic cyclin forcing using a methionine-regulated *MET3-CLN2* construct, daughter cells phase lock for a range of forcing frequencies faster than their natural cycle time, and decrease their size to do so. Mother cells lock intermittently over a higher and partially overlapping frequency range, but occasionally phase slip and initiate the cell cycle faster than the external forcing. As a result, upwards of 80% of the cells in a growing colony can be made to initiate their division cycles in synchrony.

A topological model of the cell cycle that includes only the phase and volume as variables together with a simplified size control mechanism explains our experimental results. Locking is intimately tied to the mechanism of size control. Experimentally and in the model, phase locked daughter cells implement size control during the budded period of the cell cycle and not before budding as in unforced cells. This suggests a ubiquitous mechanism of size control, revealed by the forcing. Temporal variability is also reduced in the locked state. Thus, characterizing the behavior of the cell cycle oscillator under periodic forcing reveals important aspects of its plasticity, dependence on cell size, and resistance to noise.

Author contributions: G.C., F.R.C., and E.D.S. designed research; G.C. performed research; G.C., F.R.C., and E.D.S. analyzed data; and G.C., F.R.C., and E.D.S. wrote the paper.

The authors declare no conflict of interest.

This article is a PNAS Direct Submission.

[1]To whom correspondence should be sent at the present address: Laboratoire Jolliot-Curie, Ecole Normale Superieure, 46 Allee d'Italie, 69007 Lyon, France. E-mail: gcharvin@rockefeller.edu.

This article contains supporting information online at www.pnas.org/cgi/content/full/0809227106/DCSupplemental.

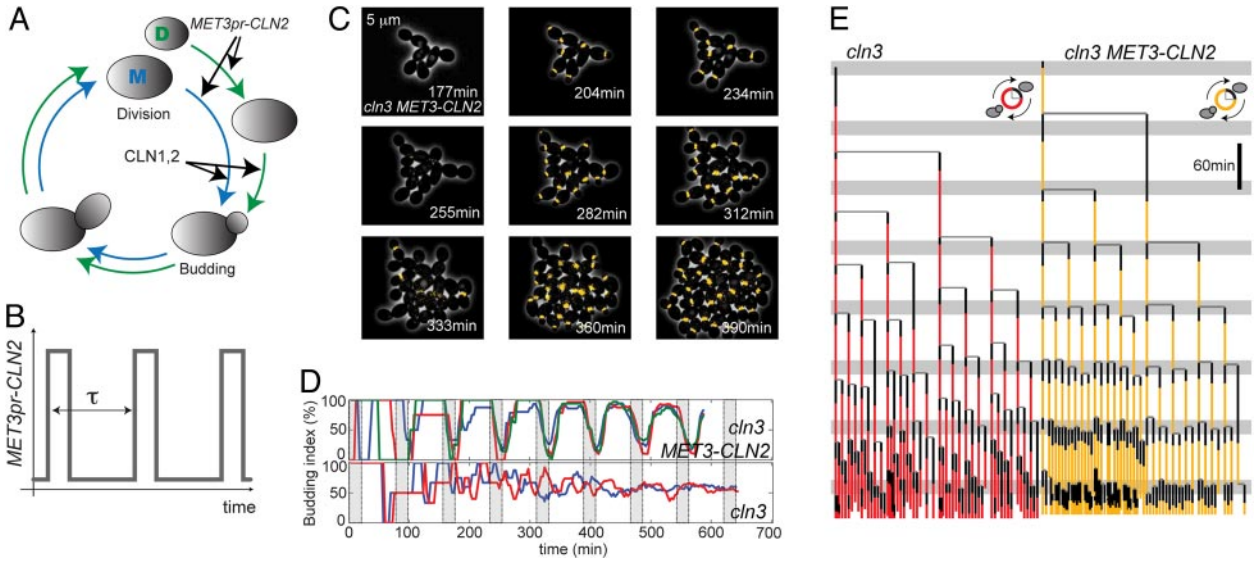

Fig. 1. Inducing synchrony in a population of cells. (*A*) Principle of the phase locking experiment. During the yeast cell-cycle, the formation of the bud is triggered by the activation of the G_1 cyclins *CLN1* and *CLN2*. Daughter cells (D) have an increased unbudded period compared with mother cells (M), because their size at division is smaller. Inducing an externally controlled pulse of *CLN2* (*CLN2* driven by the *MET3* promoter) artificially triggers budding. (*B*) Principle of the forcing. A 20-min pulse (repeat period τ) of *CLN2* was achieved by transiently activating the *MET3* promoter in a flow cell. (*C*) Sequence of images obtained during a time lapse assay under forcing conditions (period of forcing $\tau = 78$ min) in the microfluidic device, showing an overlay of phase and YFP fluorescence signal from the *CDC10-YFP* protein that stains the bud neck of budded cells. Each row of 3 images advances by 1 pulse period. (Scale bar: 5 μm.) (*D*) Budding index of growing colonies as a function time for locked (*cln3 MET3-CLN2*) and control cells (*cln3*). Each solid colored line represents an independent colony. The gray areas indicate the position of the pulse. (*E*) Pedigree tree of a growing colony of locked (black/orange) and control cells (black/red). The black segment represents the unbudded period of the cell whereas the colored one is the budded period. Gray stripes show the position of the pulse.

Results

In budding yeast, 3 G_1 cyclins, Cln1, Cln2, and Cln3, promote the transition from G_1 to S and at least one is required for viability. Cln3p functions primarily as an activator of transcription of the redundant homologous gene pair encoding Cln1 and Cln2. After initial activation by Cln3, Cln1 and Cln2 then drive their own transcription via a positive feedback loop, trigger budding, and indirectly control the onset of DNA replication (see Fig. 1*A*) (13, 14). Studies have shown that a short exogenous pulse of *CLN2*, transcribed from the inducible *MET3* promoter, can reliably trigger the G_1/S program in a strain where all endogenous G_1 cyclins were deleted (*cln1 cln2 cln3*) (12). The *MET3* promoter is sharply activated upon methionine depletion but is firmly repressed when methionine was added back to the medium. Because the media can be changed in 1 minute in our flow cell, and the lifetime of Cln2p is 5–10 min (vs. a doubling time of 84 min) we can apply very localized pulses of Cln2p. Furthermore, the G_1 cyclins have no known effect outside of G_1, because complete removal of G_1 cyclins in cycling cultures allows ongoing post-G_1 cell cycles to complete on schedule, followed by quantitative G_1 arrest after mitosis. It is also important to note that the *MET3-CLN2* construct has been calibrated to produce a level of transcription comparable to the endogenous *CLN2* promoter (12); therefore, we should avoid overexpression artifacts in this work.

To amplify the regime where phase locking might occur, we slightly modified the architecture of the G_1/S transition network by knocking out *cln3* to down-regulate the endogenous signaling that triggers the G_1/S transition. *CLN1* and *CLN2* transcription still activate and drive positive feedback in the absence of *CLN3*, but this occurs with a substantial delay in both mother and daughter cells (9, 15). Despite the longer G_1 duration of *cln3* mutant cells than that in WT, *cln3* mutant cells bud and divide normally and have the same mass doubling time as WT cells (15, 16).

In an attempt to lock the cell cycle, we made periodic 20-min-long pulses of exogenous *CLN2* in dividing *cln3 MET3-CLN2* cells (Fig. 1*B*). Asymmetric division causes new daughter cells to have a division time that is intrinsically longer than mothers (respectively 94 min vs. 71 min in our apparatus), primarily because of the smaller birth size of daughters and a size control mechanism that delays budding in small cells (Fig. 1*A*) (9). Following previous theoretical work on cell cycle phase locking (11), we tried to lock the daughters, using a forcing period $\tau = 78$ min, that is smaller than their natural division time.

Single cells were trapped in the microfluidic device previously described, in which they could grow for ≈8–10 generations while remaining perfectly flat (see image sequence in Fig. 1*C*) (12). Using semiautomated annotation software, we could retrieve cell contours from phase contrast images and budding and division timings using the fluorescent *CDC10-YFP* budneck marker (see Fig. 1*C*) (12, 15). Strikingly, forced cells (both mothers and daughters) exhibited a high level of synchrony in phase with the externally controlled *CLN2* pulses, budding ≈30 min after the pulse start in each cycle. A quantitative measure of this synchrony is the budding index (the fraction of budded cells in the colony) of these *cln3 MET3-CLN2* cells, which displayed strong sustained oscillations (Fig. 1*D Upper* and Movie S1) with a period and phase matching that of the pulse (shaded area in Fig. 1*D*). Control *cln3* cells lacking *MET3-CLN2* (Fig. 1*D Lower* and Movie S2) did not display a collective oscillation, indicating that the effect was specifically because of *MET3-CLN2* induction. Visual inspection of the colony pedigree tree further supported the idea that forced *cln3 MET3-CLN2* cells but not control *cln3* cells divided synchronously and in phase with the external pulse (Fig. 1*E*). Interestingly, the same experiment procedure carried out with *MET3-CLN2 CLN3*$^+$ cells displayed a much lower level of synchrony (see Fig. S1), probably because the endogenous *CLN3* activates *CLN1,2* before the external pulse arrives when $\tau = 78$ min.

Observing collective oscillations across the whole colony was surprising because it implied that mother cells, despite their natural fast 71-min division time, slowed down their cycle to match the period of the external pulse. To analyze this further, we conducted the same experiment with $\tau = 90$ min, which is close to the natural

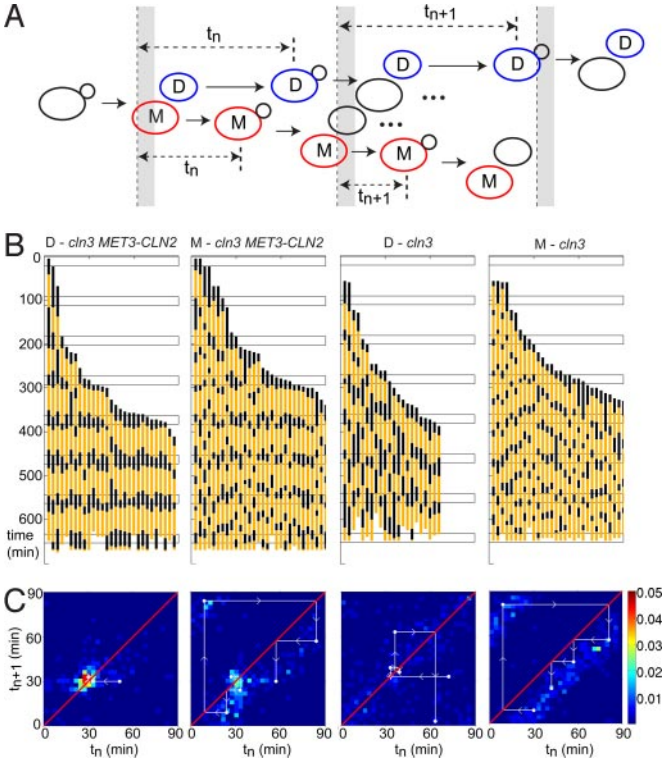

Fig. 2. Phase locked trajectories and return maps. (*A*) Schematic of how data are collected to follow a single mother cell or successive daughters relative to the periodic forcing for several generations. The gray bar indicates the cyclin pulses. (*B*) Budded (orange) and unbudded (black) intervals for the multigeneration data for the indicated genotypes for mothers (M) and successive daughters (D) and a forcing period of $\tau = 90$ min. The open bars show the cyclin pulses. (*C*) Scatter plots or putative return maps (see text) of successive intervals t_n as defined in *A* for the data in *B*. The number of data points in each bin is displayed with a color histogram. Successive values for a typical cell are shown as white trajectories.

daughter period and considerably slower than the natural mother period. The pedigree could be conveniently separated into two different kinds of trajectories: successive divisions of daughters (D → D) or mothers (M → M), respectively blue and red cells on Fig. 2*A*. Fig. 2*B* shows typical sequences of cell divisions obtained when following successive daughters or mothers for several generations.

To visualize the degree of locking, we make use of a "return map," in which the time from pulse to budding in one cycle t_n is compared with the time from pulse to budding in the succeeding cycle t_{n+1}, in either a D → D series or an M → M series, see Fig. 2*A*. It should be intuitively obvious that if the cycle is locked, then t_n and t_{n+1} will have the same value ("fixed point"); further, this value should correspond to the time required for the pulse of exogenously controlled *CLN2* to induce budding. Conversely, if no locking occurs (as in the trivial control case of *cln3* cells lacking *MET-CLN2*), then t_n and t_{n+1} should have no fixed relation for an asynchronous culture, because the pulse will arrive at random times relative to subsequent budding. It is less obvious but still a simple consequence of the system that in the absence of locking, if the pulsing frequency is approximately the same as the natural frequency, then the plot of t_n vs. t_{n+1} for a population of cells should be distributed along the diagonal (with variation off the diagonal due to measurement error or intrinsic cell cycle variability). If the pulsing frequency is slower than the natural frequency, the plotted t_n vs. t_{n+1} for individual cells should be on a line parallel to but below the diagonal of equality; if the pulsing frequency is faster, then t_n vs. t_{n+1} should plot on a line above the diagonal.

When plotting *cln3 MET3-CLN2* data (far left in Fig. 2*C*) for forced successive daughters, the vast majority of the points clustered in a small region of the map close to the diagonal, implying locking (≈300–400 events per map). For mothers, some points lie in the same area as daughters, but many others were spread below the diagonal of equality. This comes from the fact that mothers are former daughters that budded in phase with the pulse. It takes them a couple of generations to eventually run ahead of the force (points below the diagonal) and add a period. For the control *cln3* cells, successive daughters approximately spread all along the diagonal, indicating that their division period was close to the forcing period but there was no control on the phase and no locking. Control mother cells, as expected, divided significantly faster than the pulsing period, and occupy a uniform band below the diagonal.

Typical trajectories of successive daughter or mother cells for several generations (represented as white lines with arrows on Fig. 2*C*) emphasize the fact that steady locking is only observed with *cln3 MET3-CLN2* successive daughters (the line stays in the fixed point area). This results in synchronous divisions of successive daughters across the cell colony, which is obvious in the pedigree (see Fig. 2*B*). However, *cln3 MET3-CLN2* mothers escape the fixed point by running faster than the pulses.

How does the locking affect the dynamics of the cell cycle and the physiology of the cell? To answer this question, we compared the size of the cells (using pixel area covered by the cell profile by our automatic cell segmenter) at division and subsequent budding of the *cln3 MET3-CLN2* cells vs. the *cln3* cells, with a forcing period of $\tau = 90$ min. Both mothers and daughters were slightly smaller when locked than control cells, the effect being more pronounced for daughters (mean area at division = 550 ± 5 pixels for locked daughters vs. 600 ± 5 pixels for control daughters) (Fig. S2*a*). Cell cycle timings were also affected by phase locking: locked daughters had a shorter division time (mean division time is 89 min for locked daughters vs. 94 min for control daughters), whereas mother division time was slightly increased (Fig. S2*b*). This difference originates from a moderate decrease in daughter G_1 duration under forcing conditions as compared with the control *cln3* cells (respectively 31.5 min vs. 36 min, see Fig. S2*b*). Interestingly however, variability in this interval underwent a significant decrease for daughters cells upon forcing as opposed to control cells (the coefficient of variations (CV) were respectively 0.37 in forced cells vs. 0.52 in control), in such a way that G_1 noise for forced daughters cells became comparable to mother cells (CV = 0.37, see Fig. S2*b*).

Because the G_1 unbudded period is the time in the cell cycle when size control is exerted, while in the locked cells, timing of budding appears instead to be under control of the externally induced *CLN2* pulse, we wanted to examine size control in the locked cells. Following the methodology introduced in ref. 9, we plotted the duration of the G_1 period (multiplied by the growth rate μ) as a function of the size of the cell at division division (i.e., its size at birth, the beginning of G_1). If exponentially growing cells tightly control their size upon budding, then a semilog plot should give a slope close to −1 (as opposed to a slope of 0 in case of no size control indicating G_1 duration is independent on cell size) (9). Indeed, control *cln3* daughter cells displayed a significant G_1 size control, whereas mothers did not (Fig. S2*c*). In contrast, locked *cln3 MET3-CLN2* daughters had minimal G_1 size control. A similar plot can be constructed to look for size control in the budded period. Although no size control in the budded period was observed in control *cln3* cells, it was very evident in forced *cln3 MET3-CLN2* cells ($\tau = 90$ min) examined under identical conditions. This will be discussed further below in the context of our mathematical model.

What is the range of periods of *MET3-CLN2* pulsing over which the daughter cell cycle can be entrained? To answer this question, we repeated above experiments varying this period τ from 61 to 99 min (see Fig. 3*A* for data at 69, 78, and 90 min). The data were markedly noisy, so we operationally quantified the extent of phase locking by marking an interval 31.5 ± 10.5 on both axis of the return

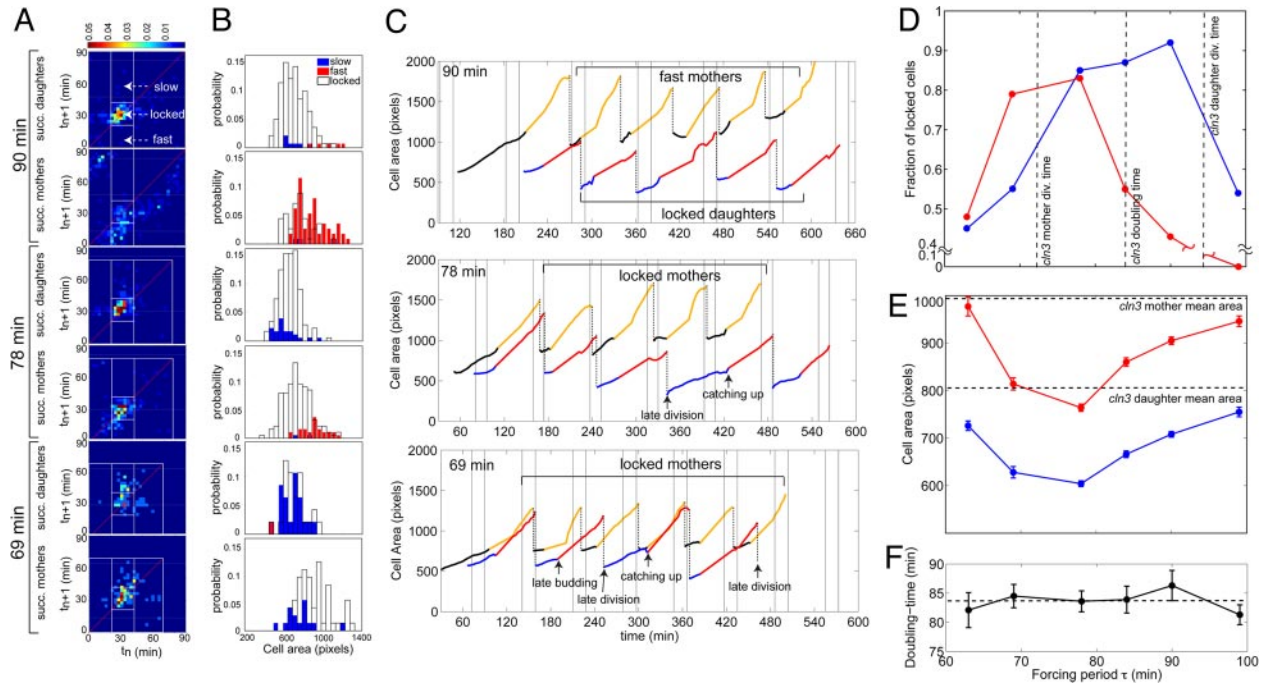

Fig. 3. Range of forcing periods. (*A* and *B*) Return maps (*A*) and histogram of cell area at budding (*B*) for successive daughter and successive mother cells forced at the indicated period. The return map is the same as in Fig. 2. The white lines delimitates the locked cells (inside the white square) from the slow cells (above) and cells that are running faster than the pulse (below). The size and position of this square is justified in the text. The histograms show the size at budding for locked (empty black bars), slow (solid red bars) and fast (solid blue bars) cells. (*C*) Examples of temporal trajectories showing the area of single cells as a function of time at different forcing periods. The black/orange traces represent successive mothers, distinguishing the unbudded (black) and budded (orange) stages of the cycle. The blue/red traces represent successive daughters with unbudded (blue) and budded (red) stages. (*D*) Fraction of locked mother (red curve) and daughter cells (blue curve) and the different locking periods. (*E*) Mean cell area at budding as a function of forcing period for daughters (blue symbols) and mothers (red symbols). (*F*) Mean colony cell doubling-time as a function of locking period. The dashed line indicates the doubling-time of unforced cells (84 min).

map of the pulse to bud interval (Fig. 3*A*). Cells within the square are defined as "locked"; "fast" cells have an abscissa within the marked interval and an ordinate below; slow cells lie above the square. The interval 31.5 ± 10.5 was chosen to match the measured time interval between the onset of the cyclin pulse and budding in the triple cyclin mutant *cln1,2,3* (12). This method is sensitive because it requires t_n (pulse-to-budding in the first cell cycle) to be potentially consistent with phase locking, and then examines t_{n+1}, the behavior of the very next cycle of the same series (whether D → D or M → M). This restricts attention to the cells most likely to exhibit some degree of locking. Using this method, we found that 92% of daughters were locked vs. 43% for the mothers at $\tau = 90$ min. Conversely, the fraction of slow and fast cells was respectively 5% and 3% in daughters (respectively 3% and 54% in mothers). Interestingly, the behavior of slow and fast cells was well correlated to their area, as can be shown on the histograms in Fig. 3*B*: The fast cells tend to be larger than the locked ones, and the slow cells smaller. This is consistent with the idea that endogenous activation of the budding program (independent of the forcing) depends on cell size control, resulting in cells escaping the control of the forcing stimulus.

Because the forcing period is varied, the fraction of locked, slow, and fast cells changed. At $\tau = 78$ min, the fraction of fast mothers dropped dramatically, whereas the fraction of slow cells in daughters was still quite low (Fig. 3*B*). At $\tau = 69$ min, most of the mothers were locked, but many of the daughters were slow. Thus, varying the period lets us determine the range at which cells could be locked. At $\tau = 78$ min, the fraction of locked cells was high in both mothers and daughters and in conformity with Fig. 1 *D* and *E*, we would say both types of cells are synchronous.

To get a closer look at the cell cycle dynamics, we plotted the evolution of cell size as a function of time for a chain of successive mothers or daughters. At $\tau = 90$ min (Fig. 3*C*), a typical recording confirms that successive mothers (black/orange segments) went significantly faster than the pulsing period (indicated as empty black bars) and their size increased at each cycle. However, the daughter chain was clearly locked and size at division was steady. At $\tau = 78$ min, mothers were locked in phase (but their size increased, Fig. 3*C Middle*), and occasional mothers added a cycle. At $\tau = 78$ min, daughters were locked for the first couple of divisions. However, by the 3rd cycle the cell was small and size control during the budded period forced the cell to miss 1 cycle of the force before catching up and budding again ("late division" mark on Fig. 3*C*). In such cases, the daughter size decreases while its timing is locked to the forcing stimulus but resets during the long G_1 period that follows when the Cln2 pulse is "skipped" or "ignored" because it occurs at an unresponsive phase of the cell cycle.

The return map obscures this type of event, because we are plotting successive times for all cells (rather than 1 cell for several generations), but it does allow the conclusion that on average daughters slip behind the force whereas mothers skip ahead at $\tau =$ 78 min. (Another way of assessing locking in the 78-min data are shown in Fig. S3 and discussed below.)

To summarize all of the forcing experiments with τ ranging from 61 min to 99 min, we plotted the fraction of locked cells as a function of the forcing period, as defined from the return maps (Fig. 3*D*). Mother and daughter have different locking intervals, but they seem to overlap at $\tau = 78$ minutes, resulting in a high synchrony across the cell population. Fig. 3*E* displays the average size at budding of mothers and daughters as a function of the forcing period. In the regime where daughters lock, their average mass at budding (as well as the mother mass) was an increasing function of the forcing period. However, when the forcing period is reduced below the locked regime and cells desynchronize, cell size increases to that of the unforced cells. This unintuitive dependence of cell size

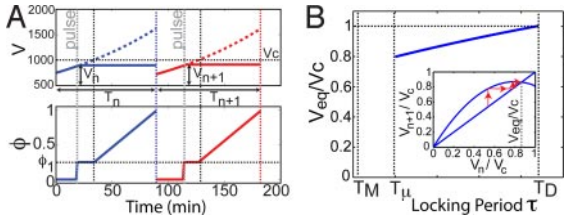

Fig. 4. A model for cell-cycle phase locking. (*A*) Time traces for volume V (*Upper*) and phase ϕ (*Lower*) of successive daughters (solid colored lines) according to the model. After the pulse (gray dashed line) all new mass goes to the bud and the total cell mass is dashed. See *SI Appendix* for parameter values. (*B*) The volume at budding (or pulse) for phase locked daughters as a function of forcing period over the locked range. (*Inset*) Convergence of the cell volume at successive pulses to the fixed point V_{eq}.

on forcing period is well captured by our model (see below). In striking contrast, over the whole range of forcing period, the overall cell doubling time across the whole colony (≈84 min) keeps remarkably constant (within 5%) and is similar to the one of unforced cells (see Fig. 3*F*). Thus, the pulse skipping/catching up events and late budding appear to compensate for the perturbation induced by the forcing, to yield an overall average cell doubling time closely matching the probable mass doubling time. Therefore, even under these circumstances the rule that "growth is limiting for division" is still followed (7).

Model. Previous models of the cell cycle (17) are too cumbersome to apply to a population of cells even when generalized to permit phase locking (11). The essence of our observations can be semi-quantitatively understood by a simple model (see *SI Appendix* for details) that describes the progression of the cell cycle as a single phase variable ϕ ($0 < \phi < 1$). The phase ϕ of exponentially growing cells (volume V, overall doubling-time μ) increases linearly with time at the rate ω. We introduce the coupling between growth and division by assuming that the phase increases less rapidly in small cells (i.e., those smaller than a critical volume V_c):

$$\frac{d\phi}{dt} = \omega \frac{V^m}{V^m + V_c^m} \quad [1]$$

$$\frac{dV}{dt} = \mu V \quad [2]$$

where m characterizes the strength of coupling between V and ϕ. For simplicity, we only consider the case of an ideal size control $m \to \infty$, which permits an analytical solution. Under these assumptions, big cells ($V > V_c$) have a division time $T_M = 1/\omega$, whereas small cells ($V < V_c$) experience a delay (division time T_D) that depends on their size at birth. We define ϕ_1 as the phase at which the cell undergoes budding. After budding, we assume that all of the newly created mass goes to the daughter. This set of rules uses only 2 variables and 3 nontrivial parameters (V_c only defines size units), all of which can directly be determined from the single cell datasets. Yet it qualitatively capture the essential features of the yeast growth and division process such as asymmetry in mother/daughter cell size and G_1 timings, and G_1 size control (see *SI Appendix*).

Cells respond to a pulse (assumed instantaneous) of exogenous cyclin by resetting their phase to ϕ_1 if they are in G_1 but ignore the pulse if they are already budded (Fig. 4*A*).

Under this set of assumptions, successive daughters converge to a state locked to the periodic external pulse provided that τ is chosen in the interval $[T_\mu; T_D]$, where $T_\mu \equiv \log(2)/\mu$ is the overall mass doubling time. This theoretical interval is quite consistent with experimental data, because daughter locking is observed between ≈78 min and 90 min (mass doubling time is 84 min, and daughter division time is 94 min).

Locking implies that (*i*) the phase is synchronized to the pulse ($\phi = \phi_1$ right after the pulse), (*ii*) the division time converges to τ and (*iii*) the cell volume just after the pulse (or equivalently at budding) converges to (see *SI Appendix* for the derivation of this formula):

$$V_{eq} = V_c e^{\mu(1-\phi_1)/\omega}(1 - e^{-\mu\tau}); \quad [3]$$

V_{eq} is an increasing function of τ (see Fig. 4*B*), as indeed observed experimentally (Fig. 3*E*). Over the whole locking interval, the cell size can vary up to 20%, which is of the same order of magnitude as the variation observed in the experiments between τ = 78 min and τ = 90 min (Fig. 3*E*).

More strikingly, the duration of G_1 does not depend on the size at division, because budding is controlled by the external pulse. In this sense, G_1 size control is abolished. However, as noted above, the model predicts that, among triggered cells, those that have not yet converged to the locked state (characterized by $V_{bud} = V_{eq}$) have a budded duration that depends on their size at budding (see Eq. **16** in *SI Appendix*). Such a displacement of the size checkpoint from G_1 to $S/G_2/M$ is indeed observed experimentally in forced cells (Fig. S2*c*).

The model qualitatively describes the locking of successive daughters but appears to predict that mothers will not lock because their mass increases in each cycle. Irrespective of the model, how can mothers, whose natural division time is 71 min seem to lock to a longer period (78 min in Fig. 1 *D* and *E*)? The answer lies in the population structure. Forced daughter cells bud at a size smaller than V_c (because of the pulse) and thus stay below this threshold at division as first generation mothers. Therefore, their subsequent budding(s) is(are) triggered by the cyclin pulse, so these mothers appear locked as well (and therefore have a longer division time than the larger unforced mothers). Depending on the period of the pulse, it may take them several divisions before they reach the critical size V_c that lets them bud autonomously. Fig. S3 indeed strongly supports this idea: Forcing decreases the daughter size at birth, thus creating small first generation mothers, which need 4 generations to reach the critical size of 800 pixels needed for autonomous budding.

The qualitative description of M → M trajectories in the experimental results fits well with this explanation, because the mother cells that fell on the apparent fixed point in Fig. 2*C* were precisely the early-generation mothers; with increasing generation number these cells left the fixed point and populated the fast region under the diagonal.

Discussion

We have unambiguously induced phase locking in the daughter cells of an exponentially expanding yeast population over a range of periods. Because in this experimental system, we can only add cyclin, not remove it, the external "force" can only shorten the period, not lengthen it. For daughters, the budding time not only comes into synchrony with the external clock, but the mass at budding is also fixed. External control of the Start transition substantially decreases temporal variability in the cell cycle in part by circumventing the naturally noisy positive feedback activation of *CLN1,2* (9, 14). Mothers only transiently lock, they are born in phase, but their mass at budding increases and they occasionally skip ahead of the external pulse (increase in size of mothers at each generation is a simple consequence of continued exponential growth of cell mass, combined with a nonzero unbudded period). Nevertheless, at τ = 78 min, more than 80% of cells in a population bud in phase, including a substantial fraction of the mothers. This clarifies the distinction between the mathematical treatment of phase locking, where a single oscillator is followed over many periods and what happens in an expanding yeast population.

There is a fundamental distinction between phase locking, which is a generic property of nonlinear oscillators, and a periodic block-release experiment, such as we did in ref. 12. Phase locking

requires stable oscillations in the absence of any external influences, which are then entrained by a periodic perturbation. The generality of this result, and thus the stability of the locked state against noise, requires nonlinearity in the underlying oscillatory mechanism.

The traditional way to obtain a population of cells in cell cycle synchrony, is to block the cell cycle and wait approximately 1 cycle time for all cells to accumulate at the block (6). Growth continues and upon release synchrony lasts for 2 generations or less, with potential artifacts from the block. Our phase locking protocol is a less invasive way of synchronization (methionine concentration has a negligible effect on growth rate), if a technical means can be found to impose it on liquid cultures. This could be achieved, for example, if a gene inducer could be found that was highly labile, so that periodic addition to a batch culture would result in only very transient gene induction across the population.

The nonintuitive changes in the mother-daughter sizes, the interval of locking periods, and the mother phase slips seen with periodic forcing in Fig. 3 are all accounted for semiquantitatively by an extremely simple model. The cell cycle is reduced to a single phase whose rate of increase is size dependent, complemented with the usual exponential rate of size increase. An explicit solution of this model reveals that synchrony propagates through the pedigree as a single cell expands to a colony. This treatment is complementary to models that focus on the genetic components of the oscillator (17), but ignore intergeneration effects. Our model is phenomenological, and will apply to any other way of periodically coupling to the cell cycle and any genetic background if we redetermine the 4 free parameters.

The population doubling time of our cultures is independent of the external forcing (within $\approx 5\%$), in accordance with the insight (7) that growth is independent of the cell cycle. However, forcing the cells significantly modifies the coordination between cell growth and division. Studies have quantitatively described how a G_1-specific size control mechanism operates to prevent small cells to enter a new division cycle (9). Our experiments reveal that (*i*) this G_1 size control can be disrupted by G_1 cyclin forcing and (*ii*) a similar size control mechanism becomes visible in the budded period ($S/G_2/M$) when G_1 size control is bypassed, a matter that has been a subject of some debate (18, 19). Intriguingly, some results in fission yeast (20) suggest the converse situation: Cell size control normally occurs in G_2 in fission yeast, but cryptic G_1 size control was revealed in cells forced to divide at small size.

Our model requires that the cell cycle run slower in small cells, irrespective of whether the cells are budded. Restricting size control to G_1 should result in progressively smaller daughters when subject to periodic forcing, contrary to what we observe. Thus, in contrast to the current model of a size checkpoint, where a specific G_1 signaling pathway transduces cell size and delays Start, our study suggests any mechanism linking progression through the cell cycle (e.g., limiting Cdk activity by growth controlled translation) could explain how yeast regulate their size.

We have achieved locking by pulsing *CLN2* because it is naturally very unstable, only affects the cell cycle in a limited window, and directly controls cell cycle progression via a well understood pathway. Our *cln3* background plausibly facilitated locking (these cells are larger than WT) and enhanced the contrast with unforced controls [*cln3* deletion augments the timing noise (15), which the locking then suppresses]. Pulsing *CLN3* itself also leads to locking in model calculations (11), but *CLN3* is subject to complex translational control and is more ubiquitous than *CLN2*. Whether locking can be achieved by pulsing the genes controlling mitotic entry or exit (e.g., *CLB2* or *CDC20*) could constitute an interesting extension to our study (11). Understanding which components of the cell cycle oscillator are most amenable to locking may indeed provide clues as to how synchrony is achieved between cells such as the very regular divisions in the *Drosophila* or *Xenopus* blastula (21, 22).

Methods

Strains. All strains used are congenic to W303 and were generated by crosses and tetrad analysis. Some fluorescent markers that are present in the strains were not scored in this study. These markers do not affect the physiology of the cell (15). See *SI Appendix* for the list of strains used in this study.

Time-Lapse Experiments. These time-lapse experiments were done with the same apparatus described in ref. 12. Cells were grown overnight and diluted in the morning on the day of the experiment. The microfluidic device was assembled as reported (12), using 20 μL of O.D. 0.02 cells. Images (phase contrast and YFP fluorescence) were acquired using the MATLAB custom software XG3 every 3 min for 12 h, which corresponds to >8 generations. The sequence of media pulses was automated using a peristaltic pump and an array of electrovalves, that could be computer controlled by XG3 (12). We used standard synthetic glucose media (SCD), with (1× = 13 mM) or without (0×) methionine to control the expression of exogenous *CLN2* from the *MET3* promoter, as previously calibrated. Using a *cln1,2,3* mutant strain, we have shown that a 20-min-long pulse ensures that all of the cells experience a normal G_1/S transition (12), but, with a 10-min, pulse only 80% of the cells respond. For this reason, the duration of the pulse for forcing experiments was set to 20 min. Because the *MET3* promoter strength is approximately the same as the *CLN2* one, the expected amount of Cln2p produced must be comparable with the endogenous one.

Image and Data Analysis. All of the images were processed using custom Celltracker4 MATLAB software (12). Semiautomated cell cluster segmentation, with the help of fluorescent budneck markers, allowed us to build pedigree trees, retrieve cell area and division times. Further analysis (return maps, histograms) was done in Matlab.

For additional details and illustrations, see *SI Appendix* and Figs. S4–S7.

ACKNOWLEDGMENTS. This work was supported by the National Institutes of Health (E.D.S. and F.R.C.), National Science Foundation Grant DMR-0517138 (to E.D.S.), a cross-disciplinary Human Frontier Science Program Fellowship (to G.C.), and the Centre National de la Recherche Scientifique (G.C.).

1. Godbeter A (1996) in *Biochemical Oscillations and Cellular Rhythms* (Cambridge Univ Press, Cambridge, UK).
2. Young M, Kay S (2001) Time zones: A comparative genetics of circadian clocks. *Nat Rev Gen* 2:702–705.
3. Strogatz S (2001) in *Nonlinear Dynamics and Chaos: With Applications to Physics, Biology, Chemistry and Engineering* (Perseus, Cambridge, MA).
4. McMillen D, Kopell N, Hasty J, Collins J (2002) Synchronizing genetic relaxation oscillators by intercell signaling. *Proc Natl Acad Sci* 99:679–684.
5. Liu A, et al. (2007) Intercellular coupling confers robustness against mutations in the *SCN* circadian clock network. *Cell* 129:605–616.
6. Morgan D (2007) in *The Cell Cycle: Principles of Control* (New Science, London).
7. Hartwell L, Unger M (1977) Unequal division in saccharomyces cerevisiae and its implications for the control of cell division. *J Cell Biol* 75(Pt 1):422–35.
8. Jorgensen P, Tyers M (2004) How cells coordinate growth and division. *Curr Biol* 14:R1014–R1027.
9. Di Talia S, Skotheim J, Bean J, Siggia E, Cross F (2007) The effects of molecular noise and size control on variability in the budding yeast cell cycle. *Nature* 448:947–951.
10. Laabs T, et al. (2003) ACE2 is required for daughter cell-specific G_1 delay in S. Cerevisiae. *Proc Natl Acad Sci* 100:10275–10280.
11. Cross F, Siggia E (2005) Mode locking the cell cycle. *Phys Rev E* 72(2 Pt 1):021910.
12. Charvin G, Cross F, Siggia E (2008) A microfluidic device for temporally controlled gene expression and long-term fluorescent imaging in unperturbed dividing yeast cells. *PlosONE* 3:e1468.
13. Cross F (1995) Starting the cell cycle: What's the point? *Curr Opin Cell Biol* 7:790–797.
14. Skotheim J, Di Talia S, Siggia E, Cross F (2008) Positive feedback of g1 cyclins ensures coherent cell cycle entry. *Nature* 454:291–296.
15. Bean J, Siggia E, Cross F (2006) Coherence and timing of cell cycle start examined at single-cell resolution. *Mol Cell* 21:3–14.
16. Cross F (1988) DAF1, a mutant gene affecting size control, pheromone arrest, and cell cycle kinetics of Saccharomyces cerevisiae. *Mol Cell Biol* 8:4675–4684.
17. Chen K, et al. (2000) Kinetic analysis of a molecular model of the budding yeast cell cycle. *Mol Biol Cell* 11:369–391.
18. Harvey S, Kellogg D (2003) Conservation of mechanisms controlling entry into mitosis: Budding yeast wee1 delays entry into mitosis and is required for cell size control. *Curr Bio* 13:264–275.
19. McNulty J, Lew D (2005) Swe1p responds to cytoskeletal perturbation, not bud size, in S. Cerevisiae. *Curr Bio* 15:2190–2198.
20. Nurse P (1975) Genetic control of cell size at cell division in yeast. *Nature* 256:547–551.
21. Foe V, Alberts B (1983) Studies of nuclear and cytoplasmic behaviour during the five mitotic cycles that precede gastrulation in Drosophila embryogenesis. *J Cell Sci* 61:31–70.
22. Newport J, Kirschner M (1982) A major developmental transition in early Xenopus embryos: I. Characterization and timing of cellular changes at the midblastula stage. *Cell* 30:675–686.